THERMAL-HYDRAULIC EFFECTS OF IMPURITY DEPOSITION ON STEAM-GENERATOR TUBES OF ALFRED REACTOR

ANDREI VÎLCU [1,3], ANDREEA MOISE [1], RODICA-MARIANA ION [2]
[1] Institute for Nuclear Research (RATEN ICN) Piteşti, Romania
[2] Dept. Materials Engineering, University of Valahia, Târgovişte, Romania
[3] Doctoral School of Engineering Sciences, University of Valahia, Târgovişte, Romania
e-mail: andrei.vilcu@nuclear.ro

Abstract

In this paper, a numerical model has been developed in order to simulate thermal-hydraulic phenomena for the lead-cooled fast reactor demonstrator, ALFRED (Advanced Lead Fast Reactor European Demonstrator). This model has been applied in case of normal operating conditions which show satisfactory results that seem to be in good agreement with ALFRED parameters. These results were used in order to validate the numerical model. Also, the model has been used to simulate an air ingress accident which can cause lead oxide depositions on the steam generator. The simulation has been performed for a lead oxide deposition of 3mm on the bayonet tubes of the steam generator which shows a decrease of the steam generator performance from 36.2 MW to 14 MW.

Keywords: *Thermal-hydraulics, Lead Fast Reactor, ALFRED, Steam Generator, Lead oxide deposition*

Introduction

The use of lead (Pb) based liquid metal alloys have been proposed as candidate coolants for GEN IV fast reactors (LFR) and accelerator driven systems (ADS). Lead and lead-bismuth eutectic are promising coolants due to a series of advantages: good heat transfer proprieties, high boiling point, efficient fuel utilization, fissile material breeding and better waste management by burning minor actinides with long half-lives. Advantages cannot exist without disadvantages, so the main problems of the technology are the following: corrosion and erosion of structural materials, impurity formation and deposition and coolant reaction with air which can cause a decrease of the heat transfer performance due to flow blockage and lead oxide deposition.

At RATEN ICN there is an increased interest in lead coolant technology aimed to the construction of the lead-cooled fast reactor demonstrator, ALFRED, having a planned thermal power of 300 MWth and a thermal efficiency of 40%.

The present study addresses the thermal-hydraulic effects of impurity deposition on the steam generator (SG) tubes of the ALFRED reactor.

Geometry and main parameters for ALFRED steam generator

The main parameters for the ALFRED reactor are presented in Table 1.

Table 1. Operational parameters and materials for ALFRED

Thermal Power	300 MWth
Number of steam generators	8
Number of pumps	8
Cycle net efficiency	40 %
Steel Vessel material Cladding material SG material	SS316L 15-15Ti T91

The geometrical parameters of the steam generator [1] are shown in Table 2.

The steam generator consist of 510 coaxial tubes (bayonet tubes) arranged in a triangular lattice. Between the lead and water there is a gap which consists of high conductivity thermal powder (synthetic diamond or steel) and helium. The purpose of the helium is to detect a tube rupture and its location (on the steam side or lead side) through the pressure variation measurement. Also, between the 4thand 3rdsteel shell there is an insulating material (slave tube) whose purpose is to prevent steam condensation. The thermal resistance of this insulator being large, the heat transfer between water and steam can be neglected. The axial and the radial cross section of the bayonet tubes are presented in Figs. 1 and 2, respectively.

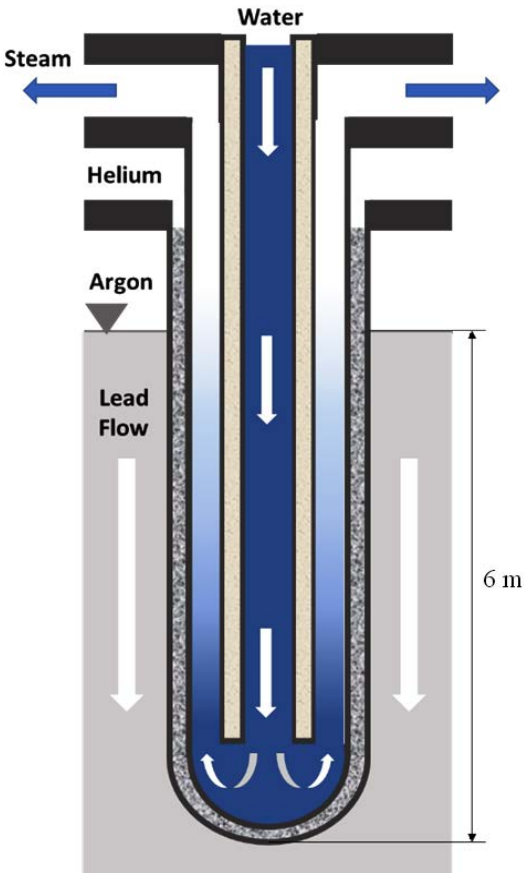


Fig. 1. Axial cross section of a bayonet tube

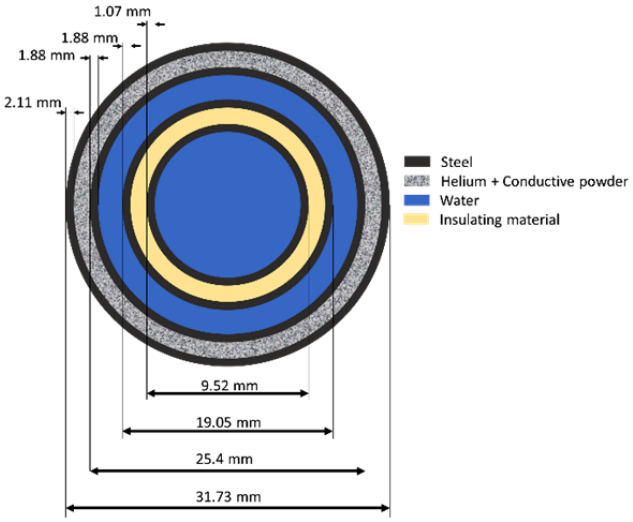


Fig. 2. Radial cross section of a bayonet tube

Table 2. Steam generator geometry

Heat exchange length	6 m
Number of bayonet tubes	510
P/D (triangular lattice)	1.42
Steam generator diameter	1.07 m

Table 3 contains the main thermal-hydraulic parameters of the steam generators. The expected thermal power extracted by a single steam generator is 37.5 MW for a lead mass flow-rate of 3247.5 kg/s and a water mass flow-rate of 24.1 kg/s, respectively.

Table 3. Main thermal-hydraulic parameters

Lead inlet temperature in SG	480 °C
Lead outlet temperature in SG	400 °C
Lead mass flow-rate	25980 kg/s
Water pressure in SG	180 bar
Water inlet temperature in SG	335 °C
Water outlet temperature in SG	450 °C
Water mass flow-rate in SG	192.8 kg/s

Numerical model for bayonet tube steam generator

While developing the present numerical model, some simplifications have been made: a) heat flux flows only in the radial direction; b) pressure drops have been neglected c) the thermal conductivity of the steel and oxide are assumed as being constant with the temperature; d) uniform thickness of oxide deposition.

The finite-difference method was applied. The following energy balance equations were used:

$$dq_i = \dot{m}_{Pb} \cdot c_{p,Pb} \cdot \Delta T_{Pb} = \dot{m}_{Pb} \cdot c_{pi,Pb} \cdot \left(T_{i-1,Pb} - T_{i,Pb}\right) \quad (1)$$

$$dq_i = \dot{m}_{water} \cdot c_{p,water} \cdot \Delta T_{water} = \dot{m}_{water} \cdot \left(i_{i+1,water} - i_{i,water}\right) \quad (2)$$

Also, we have: $$dq_i = \frac{T_{i,Pb} - T_{i,water}}{R_{tot}} \quad (3)$$

The water temperature for the next discretization zone is determined by the increase of enthalpy:

$$i_{i+1,water} = \frac{T_{i,Pb} - T_{i,water}}{R_{th,tot}} \cdot \frac{1}{\dot{m}} + i_{i,water} = \frac{dq_i}{\dot{m}} + i_{i,water} \quad (4)$$

All of the water and lead thermo-physical proprieties have been determined using appropriate data: NIST database for water, and [2] for lead.

If the total thermal resistance is known, dq_i can be determined. Once dq_i is known, lead temperature for next discretization step is computed using the relation:

$$T_{i-1,Pb} = \frac{dq_i}{\dot{m} \cdot c_{pi,Pb}} + T_{i,Pb} \quad (5)$$

The SG has triangular bundle geometry, so heat transfer coefficient for lead can be calculated using the Subbotin-Ushakov correlation [3].

$$Nu_i = 7.55\left(\frac{P}{D}\right) - 20\left(\frac{P}{D}\right)^{-13} + \frac{3.67}{90}\left(\frac{P}{D}\right)^{-2} Pe^{0.19\left(\frac{P}{D}\right)+0.56} \quad (6)$$

The wall temperature on the water side can be determined once the thermal resistance of water is known:

$$T_{i,wall} = dq_i \cdot R_{i,water} + T_{i,water} \quad (7)$$

Regarding the water, the homogenous fluid model is used and the void fraction can be calculated with the equation:

$$\alpha = \frac{x_e}{x_e - \frac{\rho_v}{\rho_l}\left(1 - x_e\right)} \tag{8}$$

The heat transfer coefficient for water varies according to the following flow regimes:

1) ***Single phase liquid flow***: when $T_{fluid} < T_{sat}$ and $T_{wall} < T_{sat}$

Being triangular lattice geometry, the Nusselt number can be computed using the following relation:

$$Nu_{\infty} = \Psi \cdot Nu_{\infty,tube} \tag{9}$$

The Nusselt number for one tube in a triangular lattice is given by the Dittus-Boelter and Weissman correlations:

$$Nu_{\infty,tube} = 0.023\, Re^{0.8}\, Pr^{0.333} \tag{10}$$

$$\Psi = 1.130\frac{P}{D} - 0.2609 \tag{11}$$

Thus, based on the above equations, the heat transfer coefficient can be calculated:

$$h_i = \frac{Nu_{\infty} \cdot \lambda_l}{D_{hidr}} \tag{12}$$

$$R_{i,water} = \frac{1}{h_i \pi D_{ext,Pb} d_{step}} \tag{13}$$

2) ***Subcooled boiling***: when $T_{fluid} < T_{sat}$ and $T_{wall} > T_{sat}$

To determine the heat transfer coefficient the modified Chen correlation is applied [4].

$$h_{t,f} = F \cdot h_{f,c} + S \cdot h_{nb}\frac{T_p - T_{sat}}{T_p - T_f} \tag{14}$$

$$h_{f,c} = \frac{Nu_{\infty} \cdot \lambda_l}{D_{hidr}} \tag{15}$$

$$h_{n,b} = 0.00122\left(\frac{\lambda_l^{0.79} c_{p,l}^{0.45} \rho_l^{0.49}}{\sigma_l^{0.5} \mu_l^{0.29} H_{lg}^{0.24} \rho_g^{0.24}}\right)\Delta T_{sat}^{0.24} \Delta p_{sat}^{0.75} = \sqrt[\Delta T_{sat}]{\frac{q''_{avg}\left(\frac{MW}{m^2}\right)}{1.97 \cdot 10^3 \cdot e^{0.23 \cdot p(MPa)}}} \quad \left(Thom\ correlation\right) \tag{16}$$

$$\Delta p_{sat} = \frac{\Delta T_{sat} \cdot H_{lg}}{T_{sat} \cdot \left(v_{i,g}\left(T\right) - v_{l(sat)}\right)} \tag{17}$$

$$F = 1,\ for\ \frac{1}{X_{tt}} < 0.1 \tag{18}$$

$$F = 2.35\left(\frac{1}{X_{tt}} + 0.213\right)^{0.736},\ for\ \frac{1}{X_{tt}} > 0.1 \tag{19}$$

$$\frac{1}{X_{tt}} = \left(\frac{x}{1-x}\right)^{0.9}\left(\frac{\rho_l}{\rho_g}\right)^{0.5}\left(\frac{\lambda_g}{\lambda_l}\right)^{0.1} \tag{20}$$

$$S = \frac{1}{1 + 2.53 \cdot 10^{-6}\Re},\ \text{with}\ \Re = Re_l\, F^{1.25} \tag{21}$$

$$R_{i,water} = \frac{1}{h_{i,tf} \pi D_{ext,Pb} d_{pas}}$$

3) ***Saturated boiling***: when $T_{fluid} = T_{sat}$ and $T_{wall} > T_{sat}$, and $x_e > 0$

In this case, the Chen correlation is used [5].

$$h_{t,f} = F \cdot h_{f,c} + S \cdot h_{nb} \tag{22}$$

Given that $x_e > 0$, for $h_{f,c}$ the below relation is applied:

$$h_{f,c} = 0.023\left(\frac{G\left(1-x\right)D_{hidr}}{\mu_l}\right)^{0.8}\left(\frac{\mu_l \cdot c_{p,l}}{\lambda_l}\right)^{0.4}\left(\frac{\lambda_l}{D}\right)F \tag{23}$$

$$R_{i,water} = \frac{1}{h_{i,tf} \pi D_{ext,Pb} d_{pas}}$$

4) ***Post-Dryout region***: when $T_{fluid} = T_{sat}$ and $x_e < 1$

To determine where the Dryout occurs, the Groeneveld Look-Up-Table [6] has been used and a diameter correction has been applied for this specific case. Thus, the value of the heat flux on the onset of Dryout can be computed according to the following relation:

$$q''_{predicted}\left(D_{exp}, p, G, x\right) = FTC\left(8, p, G, x\right)\left(\frac{D_{hidr,bayonet}}{8}\right)^{-0.5} \tag{24}$$

Groeneveld [7] suggested following empirical correlation to evaluate heat transfer coefficient for this flow regime:

$$Nu_g = a\left(Re_g\left(x + \frac{\rho_g}{\rho_l}\left(1-x\right)\right)\right)^b P_g^c Y \tag{25}$$

$$Re_g = \frac{GD_h}{\mu_g} \tag{26}$$

$$Y = \left(1 - 0.1\left(\frac{\rho_l - \rho_g}{\rho_g}\right)^{0.4}\left(1-x\right)^{0.4}\right)^d \tag{27}$$

where: $a = 5.2 \cdot 10^{-2}$; $b = 0.688$; $c = 1.26$; $d = -1.06$

5) ***Superheated steam flow***: when $T_{fluid} > T_{sat}$ and $x_e = 1$

The Weissman and Dittus-Boelter correlations are also applied for single-phase gas flow:

$$Nu_{\infty} = \Psi \cdot Nu_{\infty,tube}$$

$$Nu_{\infty,tube} = 0.023\, Re^{0.8}\, Pr^{0.333}$$

$$\Psi = 1.130\frac{P}{D} - 0.2609\ ; \qquad h_i = \frac{Nu_{\infty} \cdot \lambda_i}{D_{hidr}}$$

$$R_{i,water} = \frac{1}{h_i \pi D_{ext,Pb} d_{step}}$$

Results

DRYOUT occurrence has been determined by intersecting the power of the control volume (local power) with the Groeneveld CHF data. Thus, according to local power and quality, the DRYOUT point is identified. SG was modeled as a counter current heat exchanger.

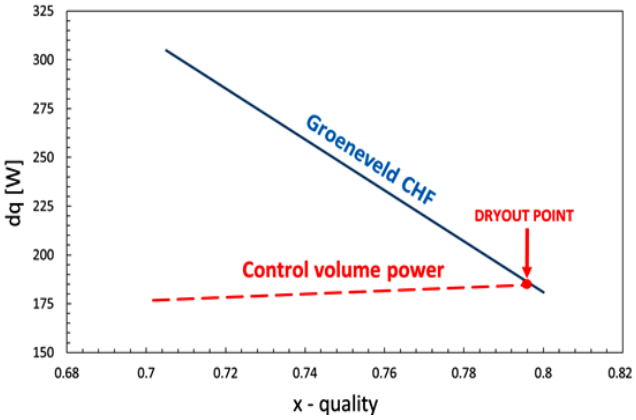


Fig. 3. Dryout point determination

In the first study, the steam generator performance has been calculated for normal operating conditions assuming an iron oxide deposition (fouling) of 100 µm.

For this case (Fig. 4), at the beginning of the heat exchange length, the wall temperature on the water side is over the saturation temperature at the respective pressure (365.99 °C for 180 bar). Thus, the modified Chen correlation for subcooled boiling has been applied.

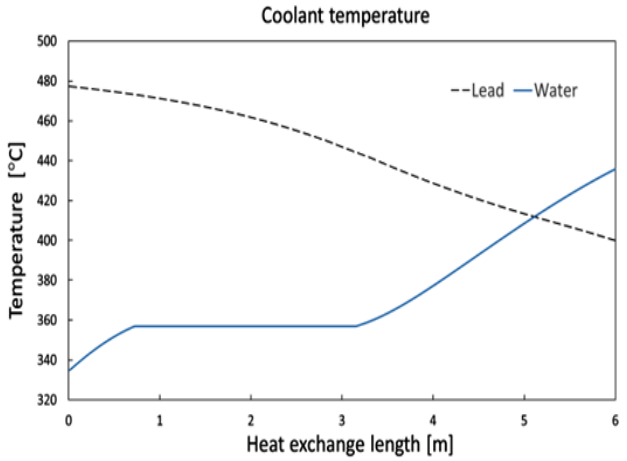


Fig. 4. Lead and water temperature over the heating length

The variation of the heat transfer coefficient for water can be seen in Fig. 5. The superheated steam flow occurs at ~ 3 m of the heat exchanger length, which is satisfactory, ensuring there are no water droplets at the SG outlet.

For this specific study, the extracted thermal power of a steam generator is 36.2 MWth, which is almost similar with the expected thermal power of ALFRED demonstrator SG (37.5 MWth).

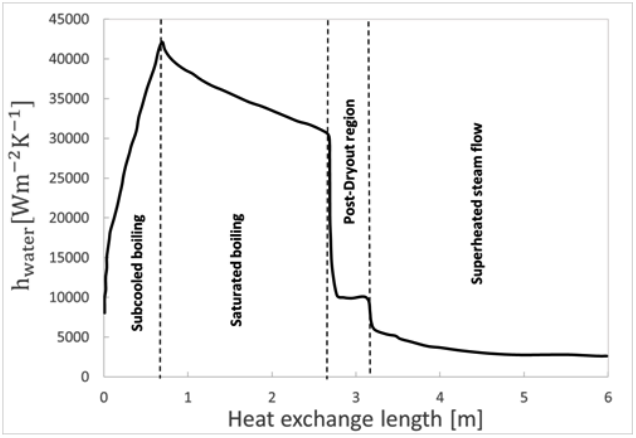


Fig. 5. Heat transfer coefficient of water

In the second study, a 3 mm lead oxide (PbO) deposition on every bayonet tube of the steam generator has been considered and the flow-rate for water and lead was kept the same as for normal operating conditions. The results obtained (coolant temperature) are presented in Fig. 6.

The thermal performance of a steam generator decreases, being able to extract only 14 MW of power. Moreover, the estimated void fraction is shown in Fig. 7, having a value of 0.8 at the outlet of the steam generator.

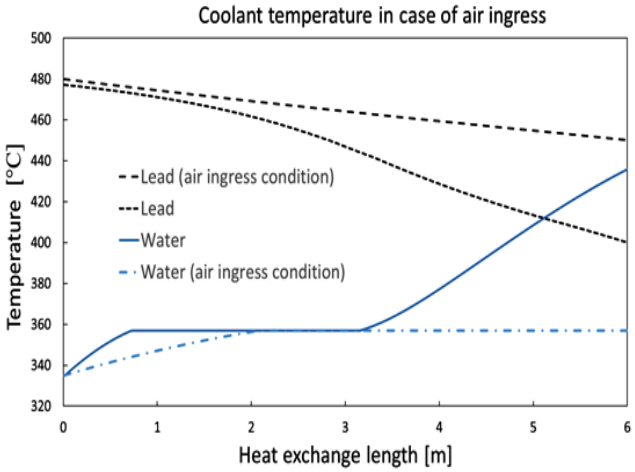


Fig. 6. Lead and water temperature in case of ingress accident

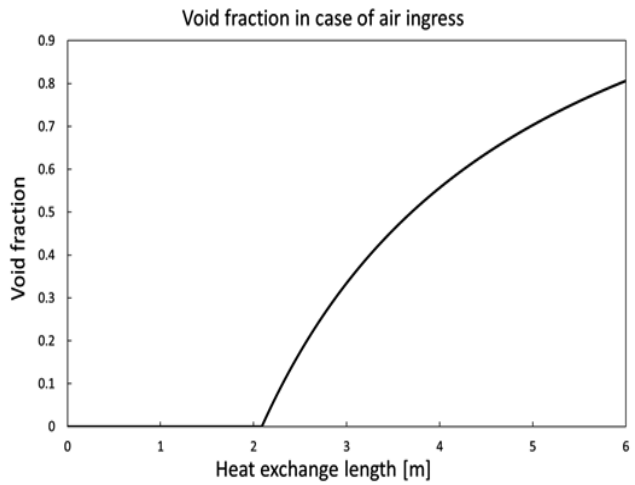


Fig. 7. Void fraction over heating length

Conclusions

A thermal-hydraulic model has been implemented to study the ALFRED bayonet type steam generator.

In normal operating conditions and assuming an iron oxide deposition of 100 μm, the extracted thermal power of the steam generators is of 290 MW, which is close to the expected thermal power of the ALFRED reactor.
In case of an air ingress accident and assuming a 3 mm lead oxide deposition on every bayonet tube of the steam generators, the performance of SGs decreases, extracted thermal power being 112 MW.

Also, the void fraction at the outlet of the steam generator is 0.8, which indicates the presence of water droplets that might damage the turbine.

These conditions might be hard to mitigate or control because of various feedback effects (e.g., deposition rate increases as the temperature of the lead decreases).

Further investigations on the following topics are needed to manage this accident type:

a) numerical and experimental analysis regarding the lead oxide deposition rate;

b) In case of a reactor shutdown, does the power decreases fast enough in order to mitigate the effects caused by the deposition?

c) In case of reactor shutdown, can the natural circulation of lead and decay heat removal system properly cool the reactor?

d) New air ingress accident mitigation and prevention systems need to be developed.

Nomenclature

Symbols [Units]

T - temperature [K]; ΔT - temperature difference [K];
w - average speed of fluid [m/s]; p - pressure [MPa];
μ - viscosity [Pa·s]; ρ - density [kg/m^3];
λ - thermal conductivity [W/(m^2 K)];
c_p - specific heat [J/(kgK)]; σ - surface tension [N/m];
v - specific volume [m^3/kg]; i - enthalpy [kJ/kg];
dq_i - power on discretization step or control volume, i [W]
q" - heat flux [W/m^2]; d_{step} - discretization step [m];
R_{th} - thermal resistance [W/K];
$\dot{m}$ - mass flow-rate [kg/s]; G - mass flux [kg/(m^2 s)];
Re - Reynolds number; Pr - Prandtl number;
Pe - Peclet number; Nu - Nusselt number;
D - diameter [m]; D_{hidr} - hidraulic diameter [m];
P/D - pitch over diameter;
Ψ - correction number for a specific lattice;
$Nu_{_tube}$ - Nusselt number for one tube;
h_{tf} - heat transfer coeff. for two phase flow [W/(m^2 K)];
h_{fc} - heat transfer coeff. of forced convection [W/(m^2 K)];
h_{nb} - heat transfer coeff. of nucleate boiling [W/(m^2 K)];
F - correction factor taking in account bubble formation in case of forced convection;
S - supression factor; ΔT_{sat} - wall superheat [K];
Δp_{sat} - pressure difference between vapors at a certain temperature and at saturation [Pa];
H_{lg} - latent heat of vaporisation [kJ/kg];
X_{tt} - Martinelli parameter; x - mass quality
x_e - equilibrium quality; SG - steam generator

Subscripts

Pb - lead; i - index for discretization step/control volume
f - fluid; p - wall; l - liquid; g - gas;
sat - saturation; ext - exterior.

References

[1] Damiani, L., Montecucco, M., Prato, A.P. (2013) ″Conceptual design of a bayonet-tube steam generator for the ALFRED lead-cooled reactor″, *Nuclear Engineering and Design*, Vol. 265, pp. 154–163

[2] Organisation for Economic Cooperation and Development – Nuclear Energy Agency (2015) ″Handbook on Lead-bismuth Eutectic Alloy and Lead Properties, Materials Compatibility, Thermal-hydraulics and Technologies″, Nuclear Energy Agency report No. 7268, Paris, France

[3] Damiani, L., Prato, A.P., Revetria, R. (2014). ″Innovative steam generation system for the secondary loop of ALFRED lead-cooled fast reactor demonstrator″, *Applied Energy*, Vol. 121, pp. 207–218

[4] Yan, J., Bi, Q., Liu, Z., Zhu, G., Cai, L. (2015) ″Subcooled flow boiling heat transfer of water in a circular tube under high heat fluxes and high mass fluxes″, *Fusion Engineering and Design*, Vol. 100, pp. 406–418

[5] Chen, J.C. (1962) A *correlation for boiling heat transfer to saturated fluids in convective flow*, United States: N. p., Web; doi:10.2172/4636495

[6] Groeneveld, D.C., Shan, J.Q., Vasić, A.Z., Leung, L.K.H., Durmayaz, A., Yang, J., Tanase, A. (2007) ″The 2006 CHF look-up table″, *Nuclear Engineering and Design*, Vol. 237 (15-17), pp. 1909–1922

[7] Groeneveld, D.C. (1975) ″Post-dryout heat transfer: Physical mechanisms and a survey of prediction methods″, *Nuclear Engineering and Design*, Vol. 32 (3), pp.283–294. doi:10.1016/0029-5493(75)90099-0